Photochemical Generation of Polymeric Alkyl-C$_{60}$ Radicals: ESR Detection and Identification

Baojun Qu,*,† Geoff Hawthorn,‡ Albert W. H. Mau,‡ and Liming Dai*,‡

State Key Laboratory of Fire Science and Department of Polymer Science and Engineering, University of Science and Technology of China, 230026 Hefei, Anhui, China, and CSIRO Molecular Science, Bag 10, Clayton South, Victoria 3169, Australia

Electron spin resonance (ESR) spectroscopy has been used to study various alkylfullerene radical adducts generated by UV-photoinitiated reactions between low-density polyethylene (LDPE) and C$_{60}$ in the presence or absence of benzophenone (BP) as a photoinitiator under different conditions. Photolysis of LDPE/BP/C$_{60}$ mixture in toluene at 323 K produced benzylfullerene (RC$_{60}$) radical adducts, showing a strong ESR signal of $g = 2.002\ 70$ with several well-resolved pairs of ^{13}C satellites. On the other hand, a well-resolved ESR spectrum characteristic of polymeric alkylfullerene (PC$_{60}$) radical adducts was observed during UV irradiation of the LDPE/BP/C$_{60}$ in benzene or in the molten state (413 K). Detailed analyses of hyperfine structures (hfs) revealed that the ESR spectrum for PC$_{60}$ radical adducts consisted of three components: (1) a broad singlet at $g = 2.002\ 50$ arising from C$_{60}$ radical anions; (2) an innermost pair of ^{13}C satellites; and (3) a 12-line spectrum superimposed on the broad singlet. Spectroscopic simulation allowed the 12-line spectrum to be attributed to the coexistence of two polymeric radical adducts of C$_{60}$ (i.e., the tertiary carbon radical adduct, $-(CH_2)_3C\text{-}C_{60}{}^{\bullet}$, designated as P$_AC_{60}{}^{\bullet}$, and the secondary carbon radical adduct, $-(CH_2)_2CH\text{-}C_{60}{}^{\bullet}$, designated as P$_BC_{60}{}^{\bullet}$), which have slightly different g values ($g_A = 2.002\ 48$ and $g_B = 2.002\ 44$) and integral intensities I_A/I_B (48.4/51.6). These results clearly indicated the generation of C$_{60}$-bonded LDPE materials simply by photoirradiation of LDPE/C$_{60}$ with BP as a photoinitiator.

Introduction

Owing to their unusual molecular structures, fullerenes and their derivatives have been shown to possess interesting electronic,[1,2] magnetic,[3,4] and photochemical[5,6] properties. In recent years, chemical modification of fullerenes and their derivatives has been exploited for making composite materials with properties characteristic of constituent components. In this regard, fullerene C$_{60}$ has been incorporated into polymeric materials through physical blending[7,8] or chemical reactions.[9,10] The combination of the unique molecular characteristics of fullerenes and good processability of appropriate polymers allows the formation of advanced polymeric materials with exotic physicochemical properties and good processability.[11] In particular, Tajima et al.[9] have used fullerene C$_{60}$ as a cross-linking reagent to effectively photo-cross-link furan-substituted polymers. The photochemical incorporation of C$_{60}$ into polymeric materials should have a wide range of potential applications, ranging from radiation curing of resins to chemical derivatization of polymers using the added C$_{60}$ as a functional group.

Fullerenes are known to undergo various addition reactions.[11,12] It was demonstrated that certain reactive free radicals (R$^{\bullet}$) can add readily onto C$_{60}$ to yield paramagnetic adducts, R$_n$C$_{60}$, which could be detected and identified by electron spin resonance (ESR) spectroscopy if n is an odd number. Using ESR as a probe, for example, Krusic et al. and Morton et al.[13−20] have successfully determined the structure of various C$_{60}$ radical

derivatives, including tri- and pentabenzyl adducts having allylic (C$_6$H$_5$CH$_2$)$_3$C$_{60}{}^{\bullet}$ and cyclopentadienyl (C$_6$H$_5$CH$_2$)$_5$C$_{60}{}^{\bullet}$ radical structures. Furthermore, these authors pointed out that such multiple addition is impossible for a bulky adduct (e.g., *tert*-butyl adduct) due to steric hindrance.[15] The addition reactions of fullerenes with free radicals, therefore, lead to not only various novel chemistries, which could be explored by ESR spectroscopy, but also a new class of fullerene derivatives.

As far as we are aware, however, ESR studies on radical adducts of C$_{60}$ have so far been mainly focused on small organic free radicals[12−20] with their polymeric counterparts being much less discussed in the literature.[21,22] Using the spin-trapping ESR spectroscopy, one of us (B.Q.) has previously investigated polymeric radicals formed by UV irradiation of low-density polyethylene (LDPE; a widely used polymer which is technologically important but unreactive for chemical modification) in the presence of benzophenone (BP) as a photoinitiator so that a fundamental understanding of the photoinitiated cross-linking of LDPE was achieved.[23,24] We have recently found that the LDPE radical intermediates thus formed could also be trapped by C$_{60}$ to produce polymeric alkyl-C$_{60}$ radical adducts. This finding should have implications not only for photo-cross-linking of LDPE but also for its chemical derivatization through the more reactive C$_{60}$ moieties. In the present paper, we report the first detailed ESR study on polymeric alkyl-C$_{60}$ radical adducts generated via the BP photoinitiated reactions of LDPE and C$_{60}$ both in solution and in the molten state.[25] ESR spectroscopic measurements and simulation allow us to assign the observed spectra and to extract structural details for the polymeric alkyl-C$_{60}$ radical adducts.

* To whom correspondence should be addressed.
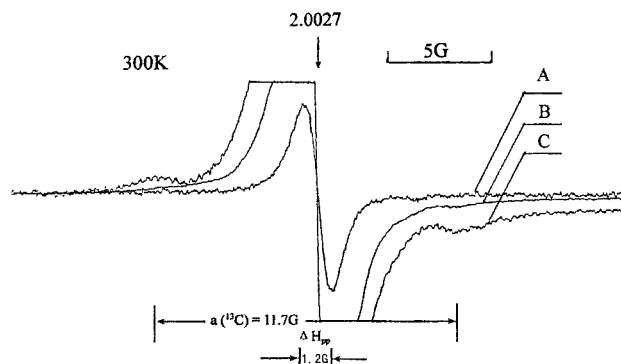† University of Science and Technology of China.
‡ CSIRO Molecular Science.

Figure 1. ESR spectra for a toluene solution of LDPE/BP/C_{60} UV-irradiated in situ at 300 K under different microwave powers (MWP) for 10 min. (A) 0.2 mW, 30 dB; (B) 20.6 mW, 10 dB; (C) 104 mW; 3 dB.

Experimental Section

Materials. LDPE 4041 resin (MI = 1.0) supplied by ICI Australia (now named Orica) was used in this work. Fullerene C_{60} (>99%) from Yin Han Hi-Tech C_{60} Co., Wuhan University, China, was used without further purification, as were benzophenone (BP, mp 47−49 °C, chemical purity from Merck), toluene, and benzene (analytical grade from Aldrich).

Sample Preparation. In a typical experiment, the LDPE/BP/C_{60}/toluene sample was prepared by dissolving 200 mg of LDPE, 4 mg of BP, and 1 mg of C_{60} in 10 mL of toluene, prepurged with dry argon, under magnetic stirring at 60 °C. The same procedure was used to prepare control samples, such as LDPE/C_{60}/toluene and LDPE/BP/C_{60}/benzene. The corresponding LDPE/BP/C_{60} and LDPE/C_{60} films for ESR measurements in the molten state were made by spreading the above toluene solutions on clean glass plates, followed by drying in a vacuum desiccator at about 70 °C until a constant weight was obtained.

ESR Measurements. ESR spectra were recorded on a Bruker ER 200D-SRC X-band spectrometer equipped with a temperature controller, accessories for UV irradiation, and readout for the magnetic field and microwave frequency. A 5 mm thin-walled Suprasil tube filled with the above-mentioned solution or film sample was placed in the cavity of the ESR spectrometer after being sealed under dry argon, and then irradiated in situ by UV light from a high-pressure Hg−Xe lamp (150 W) with a 305 nm filter. The spectrometer was operated at 9.4 GHz with a microwave power of 0.2 mW (30 dB), a modulation frequency of 100 kHz, and modulation amplitude of 100 mG. The *g* values were determined by the readout function of the spectrometer with the weak pitch as a standard, while the hyperfine splitting constants were measured using a Hall unit for calibration of the magnetic field. Simulation of the spectra was carried out on an Aspect 3000 computer attached to the Bruker ER 200D spectrometer.

Results and Discussion

Detection and Identification of RC$_{60}$ Benzyl Radicals in a Toluene Solution. *1. ESR Spectra of RC$_{60}$ Radicals in Toluene at 300 K.* Figure 1 represents the ESR spectra of a toluene solution of LDPE/BP/C_{60} recorded after UV irradiation in situ at 300 K with different microwave powers (MWP). As can be seen, the single ESR absorption (Figure 1A) with $g = 2.002\,70$ and $\Delta H_{pp} = 1.2$ G did not become saturated with an increase in the microwave power from 0.2 mW (30 dB) to 20.6 mW (10 dB, Figure 1B), and even to 104 mW (3 dB, Figure 1C). The ESR absorption increased with increasing MWP and
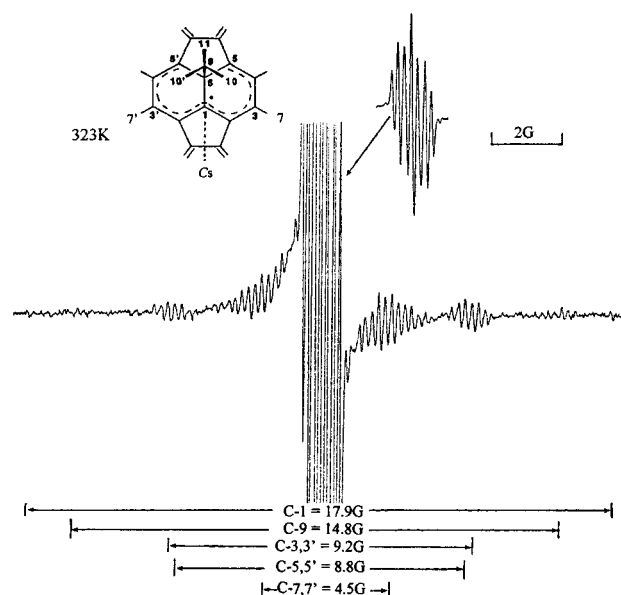

Figure 2. ESR spectrum for the LDPE/BP/C_{60} in toluene UV-irradiated in situ with a 305 nm filter at 323 K for 15 min under microwave power 0.2 mW.

decayed slowly after switching off the light. The ^{13}C satellites with the hyperfine splitting $a(^{13}\text{C}) = 11.7$ G appeared at MWP = 104 mW (3 dB, Figure 1C). After photolysis, the clear purple solution of LDPE/BP/C_{60} in toluene changed color to a light amber, most probably indicating the occurrence of a multiple addition of benzyl radicals onto C_{60} to form remarkably persistent radical anions of C_{60}. Similar spectra have been observed by photolysis of a toluene solution of C_{60} in the presence of di-*tert*-butyl peroxide.[14]

2. ESR Spectra of RC$_{60}$ Radicals in Toluene at 323 K. Figure 2 shows the ESR spectrum obtained by photolysis of the toluene solution of LDPE/BP/C_{60} at 323 K. After irradiation for a few seconds, a strong ESR signal at $g = 2.002\,70$ with several well-resolved pairs of satellites due to ^{13}C hyperfine interactions was observed. In view of the hyperfine splitting data reported for $(CH_3)_3CC_{60}{}^{\bullet}$ (17.8 G) and $^{\bullet}C_{60}CCl_3$ (18.1 G) radical adducts,[15,16] we have tentatively assigned the 17.9 G hyperfine interaction to C-1 (see structure unit in Figure 2). The 14.8 G ^{13}C hyperfine interaction, which is consistent with other γ-^{13}C hyperfine interaction of the same intensity as the outside satellites, may be attributed to C-9. The hyperfine splitting of 9.2 and 8.8 G seen in Figure 2 are close to the corresponding values of 9.4 and 8.9 G reported for $(CH_3)_3CC_{60}{}^{\bullet}$ and can be assigned to C-3, C-3′, and C-5, C-5′ (or vice versa). The 4.5 G ^{13}C hyperfine lines, possibly arising from the ^{13}C hyperfine splitting of C-7, C-7′, are relatively complex due to the overlapping of different ^{13}C nuclei. The relative intensities and hyperfine splitting of these ^{13}C ($I = 1/2$) satellite transitions in natural abundance are consistent with the anticipated C_s symmetry of the adduct radicals (see structure units in Figures 2 and 9), in which the unpaired electron locates on the two fused six-membered rings of the C_{60} surface.[14−16]

Indications for the addition of free radicals to C_{60} could also be obtained from the proton hyperfine structures. For example, the seven-line hyperfine structure (hfs) at the center (inset of Figure 2) can be assigned to the proton ^{1}H hyperfine structure of the benzyl radical adducts $C_6H_5CH_2$-$C_{60}{}^{\bullet}$, produced by H-atom abstraction of ^{3}(BP)* from toluene followed by addition onto C_{60}. The observed and corresponding simulated spectra for the proton ^{1}H hyperfine structures of the benzyl radical adducts are shown in parts A and B, respectively, of Figure 3.
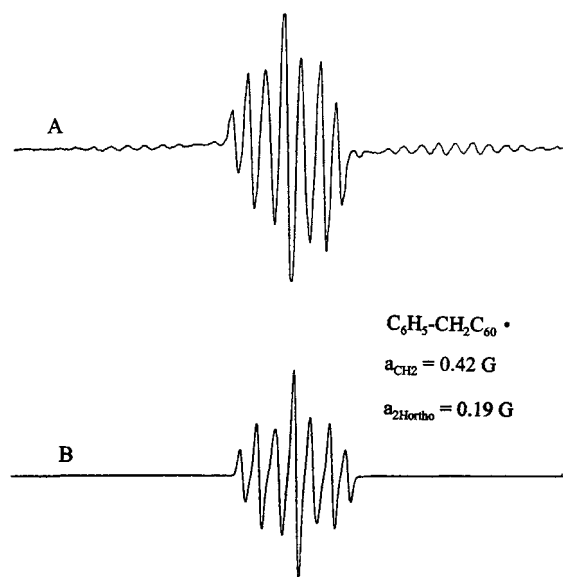
ESR Detection of Polymeric Alkyl-C$_{60}$ Radicals

J. Phys. Chem. B, Vol. 105, No. 11, 2001 **2131**

Figure 3. Observed and simulated spectra of proton ^{1}H hyperfine structures for radical adducts C_6H_5-$CH_2C_{60}$$^{\bullet}$. (A) Observed spectrum with the low gain, as shown in Figure 2; (B) the corresponding simulated spectrum with a line width parameter of 0.1 G. The ^{1}H hfs parameters used for the simulated spectrum of benzyl radicals are a_{CH_2} = 0.42 G and $a_{2Hortho}$ = 0.19 G.
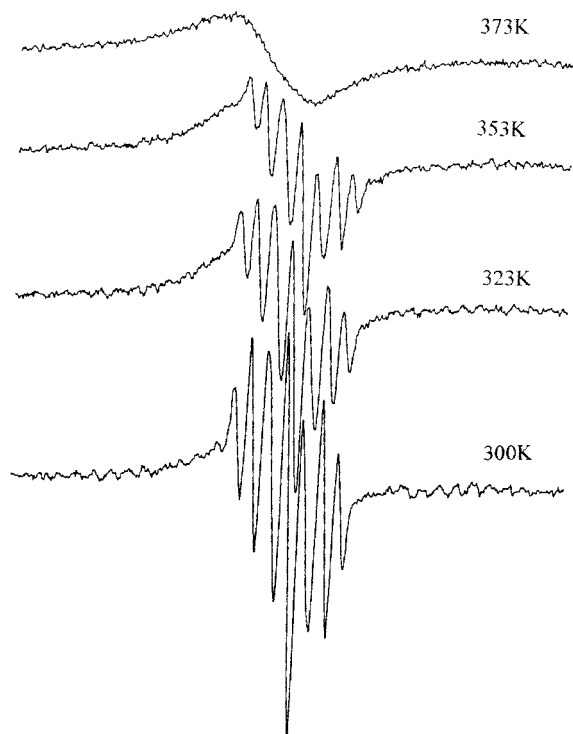

Figure 4. Changes in ESR spectra of benzyl radical adducts with increasing temperature and irradiation time. (A) 300 K, 10 min; (B) 323 K, 20 min; (C) 353 K, 40 min; (D) 373 K, 50 min.

While a 0.1 G line width was used for the simulated spectrum, the hfs parameters used were 0.42 G for two protons of the CH_2 group and 0.19 G for the two ortho protons of the benzene ring. The good agreement seen in Figure 3 further confirms the formation of benzyl radical adducts of $C_6H_5CH_2$-$C_{60}$$^{\bullet}$ by UV irradiation of the LDPE/BP/C$_{60}$ sample in toluene.

3. Temperature Dependence of the ESR Spectra for the Benzyl Radical Adducts. Figure 4 shows the ESR spectra of benzyl radical adducts recorded at various temperatures with different irradiation duration. It can be seen that the ESR intensity for
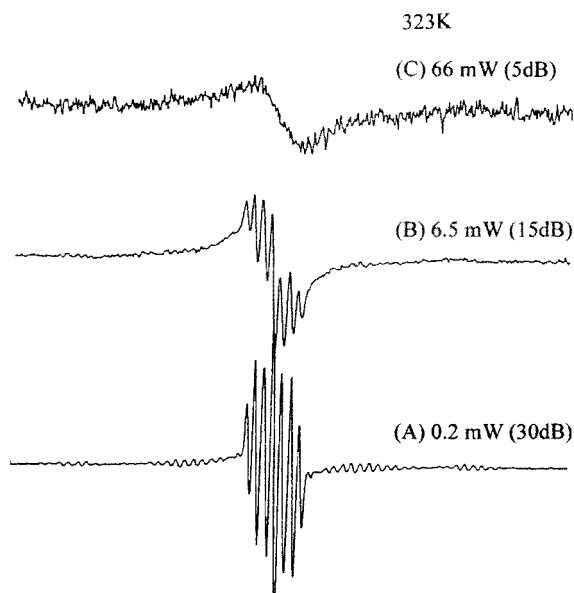

Figure 5. Changes in ESR spectra of benzyl radical adducts with increasing microwave powers at 323 K. (A) 0.2 mW, 30 dB; (B) 6.5 mW, 15 dB; (C) 66 mW, 5 dB.

the ^{1}H hyperfine structures of the benzyl radical adducts (C_6H_5-CH_2-$C_{60}$$^{\bullet}$) decreased with increasing irradiation time and temperature. Prolonged UV irradiation at 373 K caused disappearance of the ^{1}H hyperfine structures, leading to a broad spectrum. These changes indicate, once again, the occurrence of multiple addition of $C_6H_5CH_2$$^{\bullet}$ radicals onto a single C_{60} molecule.[16]

4. Microwave-Power Dependence of the ESR Spectra for the Benzyl Radical Adducts. ESR spectra of the benzyl radical adducts measured with different microwave powers at 323 K are shown in Figure 5. Unlike the broad singlet ESR spectrum shown in Figure 1, Figure 5 clearly shows the ease with which the ESR signal may become saturated with an increase in the microwave power. In particular, the ESR signals were found to decrease in intensity with increasing the microwave power from 0.2 mW (30 dB) to 6.5 mW (15 dB) and eventually become a broad, single peak at 66 mW (5 dB). Therefore, the overall absorption from the radical adducts of LDPE/BP/C$_{60}$ in toluene (Figures 1 and 5) seems to consist of at least two species: one with a rapid power saturation (benzyl radical adducts C_6H_5-CH_2-$C_{60}$$^{\bullet}$) and another more stable species (radical anion of C_{60}).

ESR Spectra of RC$_{60}$ Radicals in Benzene. ESR spectra of LDPE/BP/C$_{60}$ in benzene measured at 323 and 353K after UV irradiation at a microwave power of 0.2 mW for 10 min are given in Figure 6, which shows a 12-line hfs signal overlapped with a broad peak. Clearly, Figure 6 differs significantly from Figures 2 and 4 in that the former shows not only fewer poorly resolved hyperfine structures but also a much weaker dependence on temperature and UV irradiation. Benzene is known to be relatively inert toward *tert*-butoxyl radicals,[17] so it may be difficult to produce benzene radicals through hydrogen abstraction by the BP excited triplet state. The above observations suggest, therefore, that polymeric alkyl radicals (P$^{\bullet}$) may be produced by hydrogen abstraction of the BP excited triplet state from LDPE chains followed by addition onto C_{60} to form the PC$_{60}$$^{\bullet}$ radical adducts, along with the concomitant formation of the $C_{60}$$^{\bullet-}$ radical anions. However, the possible cross-link formation by combination of two polymer radicals (P$^{\bullet}$) cannot be ruled out,[23,24] especially in cases where C_{60} is insufficient.

Detection of Polymeric Alkylfullerene (PC$_{60}$) Radical Adducts. To test the above conjecture for the formation of
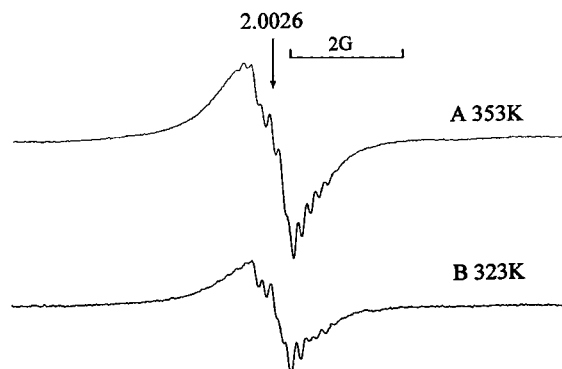
Figure 6. ESR spectra for a benzene solution of LDPE/BP/C_{60} after UV irradiation in situ for 10 min at a microwave power of 0.2 mW and two different temperatures. (A) 323 K; (B) 353 K.
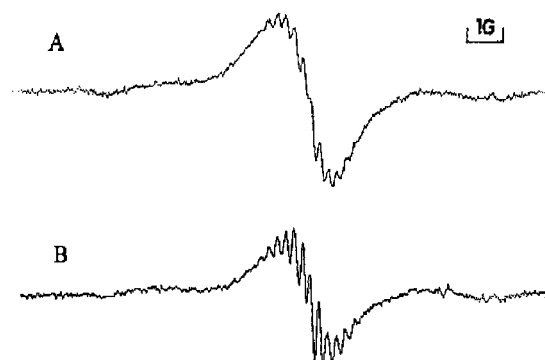

Figure 7. ESR spectra of film samples measured after UV irradiation in situ for 5 min at 413 K. (A) LDPE/C_{60}; (B) LDPE/BP/C_{60}.

polymeric alkyl-C_{60} radical adducts, we made ESR measurements on *dry* samples of LDPE/BP/C_{60} and LDPE/C_{60} after UV irradiation in the ESR cavity at 413 K for 5 min. The resulting ESR spectra are shown in Figure 7A and 7B for LDPE/C_{60} and LDPE/BP/C_{60}, respectively. Both of them showed common features of the superimposition between a signal corresponding to the 12-line hyperfine structure (hfs) and a broad singlet peak with a $\Delta H_{pp} = 1.77$ G. However, Figure 7B shows a more profound 12-line structure with a better resolution than those in Figure 7A, suggesting more polymeric alkyl radicals (P•) being added onto C_{60} in the LDPE/BP/C_{60} system due to hydrogen abstraction of the BP excited triplet state from LDPE chains. The identical *g* value of 2.002 46 measured from Figure 7 indicates that the 12-line absorption arises, most probably, from the same radical species in both cases.

Identification of PC$_{60}$ Radical Adducts. The high gain ESR spectrum for the LDPE/BP/C_{60} film recorded at 413 K after UV irradiation in situ for 5 min is given in Figure 8A, which shows the following main features: (i) a broad signal at $g = 2.002\ 46$ with $\Delta H_{pp} = 0.76$ G characteristic of $C_{60}^{\bullet-}$ radical anions produced by UV photolysis of C_{60} in the presence of donor molecules;[14] (ii) the overlapped 12-line signal associated with proton hyperfine structures from the polymeric alkyl radical adducts PC$_{60}^{\bullet}$; (iii) the appearance of ^{13}C (natural abundance 1.1%) satellite lines at high gains. However, only the innermost pair of ^{13}C satellite lines with hyperfine splitting of 5.5 G and $\Delta H = 1.1$G are observable in Figure 8A because other ^{13}C satellite lines are too weak to be detected.

Our previous studies suggest the presence of two kinds of polymeric alkyl radicals (i.e., tertiary and secondary carbon radicals) in the BP-photo-cross-linked LDPE.[23,24] As proposed in the following reaction scheme, these polymeric alkyl radicals could react with C_{60} to yield paramagnetic adducts $P_AC_{60}^{\bullet}$ and
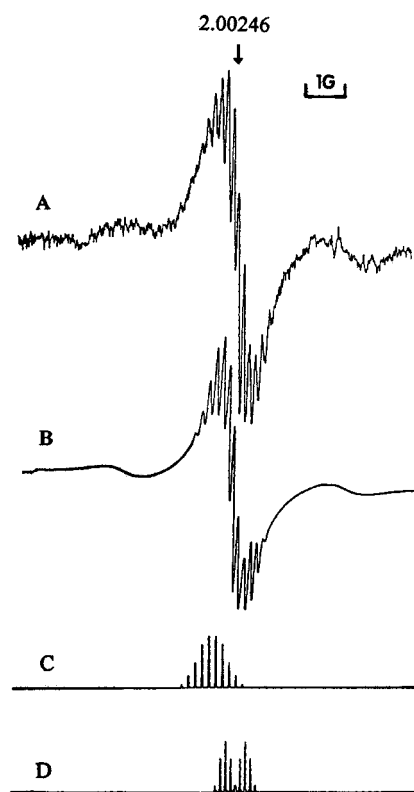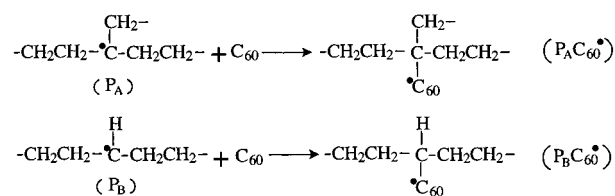

Figure 8. (A) High gain spectrum of an LDPE/BP/C_{60} film sample measured after UV irradiation in situ for 5 min at 413 K; (B) the corresponding simulated spectrum; (C) stick diagram from the ^{1}H hfs of the P_AC_{60} radical adducts; (D) stick diagram from the ^{1}H hfs of the P_BC_{60} radical adducts.

$P_BC_{60}^{\bullet}$. The $P_AC_{60}^{\bullet}$ and $P_BC_{60}^{\bullet}$ thus formed are responsible for
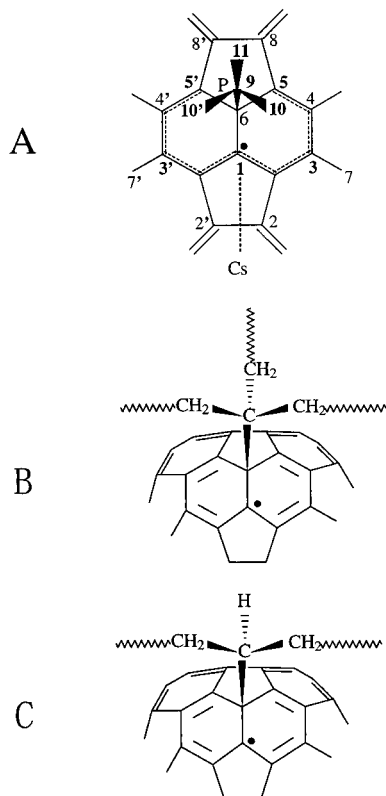

the 12-line absorption signal seen in Figure 8A, and nearly pure monoalkyl radical adducts of C_{60} are produced because of the strong steric hindrance associated with the bulky polymeric alkyl radicals.[15] The monosubstitution is reflected by the narrow line widths (ca. 80 mG) for those ESR spectra shown in Figure 8. The polymer-bound, *monosubstituted* C_{60} should provide reactive sites for further chemical derivatization.[26]

On the basis of the above analyses and the experimentally determined simulation parameters (see Figure 8A and Table 1), we derived the corresponding simulated spectrum (Figure 8B). The simulated stick spectra for $P_AC_{60}^{\bullet}$ and $P_BC_{60}^{\bullet}$ are shown in Figure 8C and 8D, respectively. The excellent agreement between the simulated spectrum (Figure 8B) and the observed spectrum (Figure 8A) indicates that the 12-line hfs signal indeed arises from the spectral overlapping between $P_AC_{60}^{\bullet}$ and $P_BC_{60}^{\bullet}$.

Prior to the present work on the polymeric alkyl-C_{60} radical adducts (PC$_{60}^{\bullet}$), several ESR studies on small organic-C_{60} radical adducts (RC$_{60}^{\bullet}$) have been reported.[13-20] Table 1 lists the simulation parameters reported in the literature,[12-14,18] along with those determined from Figure 8A. Although Table 1 shows slightly different *g* values, PC$_{60}^{\bullet}$ gives ^{1}H and ^{13}C hfs data which are very close to those of RC$_{60}^{\bullet}$ because of the localization of
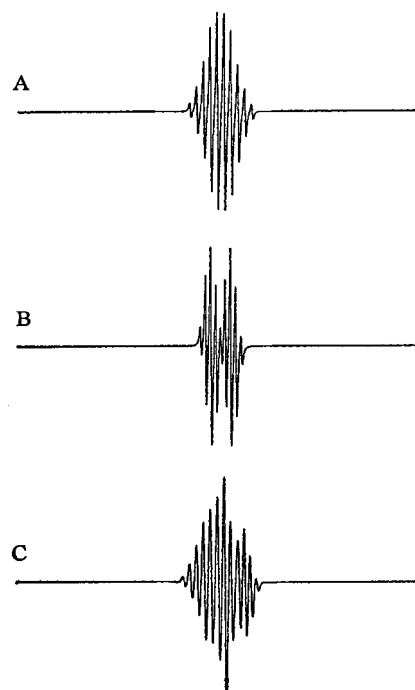
TABLE 1: Comparison of ESR Simulation Parameters Used for the Spectrum of PC$_{60}$ Radicals Shown in Figure 8B with Those Reported for RC$_{60}$[12-14,18]

P$^{\bullet}$ or R$^{\bullet}$	g factor	^{1}H	δ-^{13}C	T/K	ref
P$^{\bullet}$					
A: $-$(CH$_2$)$_3$C$^{\bullet}$	2.002 48	a(3H) = 0.34	a(3H) = 5.5	413	this work
		a(3H) = 0.17			
B: $-$(CH$_2$)$_2$CH$^{\bullet}$	2.002 44	a(1H) = 0.49	a(3H) = 5.5	413	this work
		a(4H) = 0.13			
R$^{\bullet}$					
(CH$_3$CH$_2$)$_3$C$^{\bullet}$	2.002 25	a(3H) = 0.34		350	12, 14
		a(3H) = 0.17			
(CH$_3$)$_3$C$^{\bullet}$		a(9H) = 0.17	a(3H) = 5.63	325	18
(CH$_3$)$_2$CH$^{\bullet}$	2.002 23	a(1H) = 0.48		370	13, 14
		a(4H) = 0.15			

Figure 9. Structural formula of radical adducts. (A) PC$_{60}$; (B) P$_A$C$_{60}$; (C) P$_B$C$_{60}$.

Figure 10. Simulated spectra of the 12-line hyperfine structures in Figure 8A. (A) P$_A$C$_{60}$ radical adducts; (B) P$_B$C$_{60}$ radical adducts; (C) complex spectra of (A) plus (B), assuming the intensity ratio $I_A/I_B = 48.4/51.6$ and $g_A = 2.002\,48$, $g_B = 2.002\,44$.
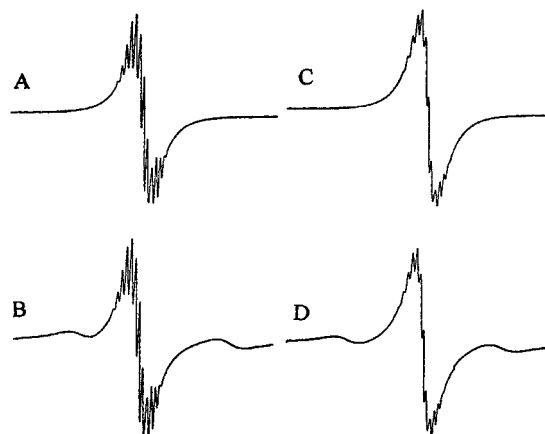
Figure 11. Simulated spectra with ^{1}H and ^{13}C hyperfine interaction. (A) Adding the broad singlet spectrum of C$_{60}{}^{\bullet-}$ radical anion to Figure 10C; (B) adding the innermost pairs of ^{13}C satellites to (A); (C) adding the broad singlet spectrum of C$_{60}{}^{\bullet-}$ radical anion to the weak signal from polymer alkyl radicals; (D) adding the innermost pairs of ^{13}C satellites to (C).

unpaired spin on the same carbon atoms of the C$_{60}$ surface, as described below.

Simulation Analyses of PC$_{60}$ Radical Adducts. Figure 9 shows structural formulas for PC$_{60}$, P$_A$C$_{60}$, and P$_B$C$_{60}$ radical adducts. As demonstrated by Morton et al.[15,16] for small molecular RC$_{60}$ radical adducts, the PC$_{60}$ radical adduct (Figure 9A) has a single plane of symmetry (C_s) passing through the carbon of the P ligand (C-9, the attacking carbon) and two carbons (C-1, C-6, the attacked carbon) on two fused six-membered rings of the C$_{60}$ surface. Before being attacked by the polymeric radical, there is a double bond between C-1 and C-6, and hence the PC$_{60}{}^{\bullet}$ radical could have an unpaired spin in a 2p orbital of C-1. The unpaired spin might confine to the three carbon atoms (C-1, C-5, and C-5′) ortho and the two carbon atoms (C-3 and C-3′) para to the attaching point of P group, as is the case for its small molecular counterparts.[16,20] The resultant radical structure having C_s symmetry, however, has most of its unpaired spin density localized on C-1 with respect to C-3, C-3′ and C-5, C-5′. However, hyperfine interactions were not restricted to the C$_{60}$ ball. Because of the

polarization and hyperconjugative effects, the ^{13}C nuclei gave rise to resolvable hyperfine structures (hfs) from the attached ligands P, as shown in Figure 9B,C.

Figures 10 and 11 show the process for simulation analyses of the observed spectrum (Figure 8A). As mentioned earlier, the 12-line signal at the center of Figure 8A is due to spectral overlapping of the proton hfs spectra of P$_A$C$_{60}{}^{\bullet}$ and P$_B$C$_{60}{}^{\bullet}$. As shown in Figure 10B, the spectrum of the secondary carbon radical $-$(CH$_2$)$_2$CH-C$_{60}{}^{\bullet}$ (i.e., P$_B$) consists of a doublet of quintuplets with a unique (0.49 G) and four equivalence (0.13 G). The tertiary carbon radical $-$(CH$_2$)$_3$C-C$_{60}{}^{\bullet}$ (i.e., P$_A$) should display septets if six protons are equivalent. However, the protons of the three $-$CH$_2-$ groups are nonequivalent due to hindered rotation around both C$_6-$C$_9$ and C$_9-$(CH$_2$)$_3-$,[16] and can be divided into two groups: one group with a(3H) = 0.34

2134 *J. Phys. Chem. B, Vol. 105, No. 11, 2001*

Qu et al.

G and another group with $a(3H) = 0.17$ G. This leads to the 10-line spectrum shown in Figure 10A due to accidental overlapping.

By assuming that P_AC_{60} and P_BC_{60} radical adducts have similar integral intensities ($I_A/I_B = 48.4/51.6$) with slightly different g values (Table 1), the simple addition of the two spectra of Figure 10A,B leads to the simulated spectrum of 12 lines in Figure 10C. The additive relationship, together with no adjustable parameters except the I_A/I_B ratio for constructing the simulated spectrum, implies, once again, that the 12-line absorption signal of Figure 8A indeed resulted from $P_AC_{60}^\bullet$ and $P_BC_{60}^\bullet$.

The simulated spectrum of Figure 11A was obtained by adding the broad singlet spectrum of the C_{60} radical anion to Figure 10C, while Figure 11B was obtained by adding the innermost pairs of ^{13}C satellite lines to Figure 11A (see Figure 8A and its associated discussion). It can be seen that the final simulated spectrum thus obtained (Figure 11B) is almost identical with that of Figure 8B and closely resembles the observed spectrum (Figure 8A). On the other hand, Figure 11C,D represents the corresponding simulated spectra for samples with insufficient amounts of polymeric alkyl radicals being added onto C_{60} molecules, which are closely related to the cases where the photoinitiator is not used (Figure 7A) or at an initial stage of the photoinitiated reactions.

Conclusions

We have demonstrated that different types of alkyl-C_{60} radical adducts (e.g., RC_{60} or PC_{60}) can be generated through UV photolysis of LDPE/C_{60} with or without BP under different conditions. In particular, benzyl-C_{60} radical adducts (RC_{60}) were observed upon the UV irradiation of LDPE/BP/C_{60} in toluene while polymeric alkyl-C_{60} radical adducts (PC_{60}) of LDPE were detected by photolysis of the same system in the relatively inert benzene solution. Photolysis of LDPE/C_{60} and LDPE/BP/C_{60} films in the molten state was also shown to generate the polymeric alkyl-C_{60} radical adducts. ESR spectroscopic measurements and simulation have, for the first time, allowed the detection and identification of the polymeric alkyl-C_{60} radical adducts (both tertiary carbon-C_{60} and secondary carbon-C_{60}) produced by photoirradiation of LDPE/BP/C_{60} in the molten state. The ease with which C_{60}-bound LDPE materials can be effectively produced simply by the photoirradiation of LDPE/BP/C_{60} blends should offer a general approach toward C_{60}-containing polymers and facilitate further chemical derivatization of the otherwise unreactive LDPE chains via various reactions characteristic of C_{60}.

References and Notes

(1) Hebard, A. F.; Rosseninsky, M. J.; Haddon, R. C.; Murphy, D. W.; Glarum, S. H.; Palstra, T. T.; Ramirex, A. P.; Kortan, A. R. *Nature* **1991**, *350*, 600.

(2) Dubois, D.; Moninot, G.; Kutner, W.; Jones, M. T.; Kadish, K. *J. Phys. Chem.* **1992**, *96*, 7137.

(3) Allemand, P.-M.; Khemani, K. C.; Koch, A.; Wudl, F.; Holkzer, K.; Donovan, S.; Gruner, G.; Thompson, J. D. *Science* **1991**, *253*, 301.

(4) Stemhens, P. W.; Cox, D.; Lauher, J. W.; Mihaly, L.; Wiley: J. B.; Allemand, P. M.; Hirach, A.; Holczer, K.; Li, Q.; Thompson, J. D.; Wudl, F. *Nature* **1992**, *335*, 331.

(5) Jehoulet, C.; Bard, A. J.; Wuld, F. *J. Am. Chem. Soc.* **1991**, *113*, 5456.

(6) Ma, B.; Lawson, G. E.; Bunker, C. E.; Kitaygorodskiy, A.; Sun, Y. P. *Chem. Phys. Lett.* **1995**, *247*, 51.

(7) See, for example: Yu, G.; Gao, J.; Hummelen, J. C.; Wudl, F.; Heeger, A. J. *Science* **1995**, *270*, 1789. Wang, Y. *Nature* **1992**, *356*, 585.

(8) Dai, L.; Lu, J.; Matthews, B.; Mau, A. W. H. *J. Phys. Chem. B* **1998**, *102*, 21.

(9) Tajima, Y.; Tezuka, Y.; Yajima, H.; Ishii, T.; Takeuchi, K. *Polymer* **1997**, *38*, 5255.

(10) See, for example: Dai, L.; Mau, A. W. H.; Griesser, H. J.; Spurling, T.; White, J. W. *J. Phys. Chem.* **1995**, *99*, 17302. Patil, A. O.; Brois, S. J. *Polymer* **1997**, *38*, 3423. Bunker, C. E.; Lawson, G. E.; Sun, Y. P. *Macromolecules* **1995**, *28*, 3744. Cao, T.; Webber, S. E. *Macromolecules* **1996**, *29*, 3826.

(11) See, for example: Hirsh, A. *The Chemistry of Fullerenes*; Thieme Verlag: Stuttgart, 1994. Wudl, F. *Acc. Chem. Res.* **1992**, *25*, 157. Dai, L. *J. Macromol. Sci., Rev. Macromol. Chem. Phys.* **1999**, *C39* (2), 273, and references therein.

(12) Taylor, R.; Walton, D. R. M. *Nature* **1993**, *363*, 685.

(13) Krusic, P. J.; Wasserman, E.; Keizer, P. N.; Morton, J. R.; Preston, K. F. *Science* **1991**, *254*, 1183.

(14) Krusic, P. J.; Wasserman, E.; Preston, K. F.; Malone, B.; Holler, E. R., Jr. *J. Am. Chem. Soc.* **1991**, *113*, 6274.

(15) Morton, J. R.; Preston, K. F.; Krusic, P. J.; Hill, S. A.; Wasserman, E. *J. Phys. Chem.* **1992**, *96*, 3576.

(16) Morton, J. R.; Preston, K. F.; Krusic, P. J.; Wasserman, E. *J. Chem. Soc., Perkin Trans. 2* **1992**, 1425.

(17) Keizer, P. N.; Morton, J. R.; Preston, K. F.; Krusic, P. J. *J. Chem. Soc., Perkin Trans. 2* **1993**, 1041.

(18) Morton, J. R.; Negri, F.; Preston, K. F. *Can. J. Chem.* **1994**, *72*, 776.

(19) Krusic, P. J.; Roe, D. C.; Johnston, E.; Morton, J. R.; Preston, K. F. *J. Phys. Chem.* **1993**, *97*, 1736.

(20) Morton, J. R.; Negri, F.; Preston, K. F. *Acc. Chem. Res.* **1998**, *31*, 63.

(21) Pace, M. D. *Appl. Magn. Reson.* **1996**, *11*, 253.

(22) Dyakonov, V.; Zoriniants, G.; Scharber, M.; Brabec, C. J.; Janssen, R. A. J.; Hummelen, J. C.; Sariciftci, N. S. *Electronic Properties of Novel Materials—Progress in Molecular Nanostructures*; AIP Conf. Proc. **1998**, *442*, 257.

(23) Qu, B. J.; Xu, Y. H.; Shi, W. F.; Rånby, B. *Macromolecules* **1992**, *25*, 5215.

(24) Qu, B. J.; Xu, Y. H.; Shi, W. F.; Rånby, B. *Macromolecules* **1992**, *25*, 5220.

(25) Part of the work has been presented at the Second Asia-Pacific EPR/ESR Symposium, Hangzhou, China, Oct 31—Nov 4, 1999.

(26) See, for example: Dai, L.; Mau, A. W. H. *Synth. Met.* **1997**, *86*, 2277.